Preliminary establishment and validation of the inversion method for growth and remodeling parameters of patient-specific abdominal aortic aneurysms

Chen Peng
Zhejiang Lab
Wei He
Zhongshan Hospital
Jingyang Luan
Zhongshan Hospital
Tong Yuan
Zhongshan Hospital
Weiguo Fu
Zhongshan Hospital
Yun Shi
shi.yun@zs-hospital.sh.cn
Zhongshan Hospital
Shengzhang Wang
Fudan University

Research Article

Keywords: Abdominal Aortic Aneurysms, Growth and Remodeling, Homogenized Constrained Mixture Theory, Inverse Method, Finite Element Simulation

Posted Date: November 1st, 2023

DOI: https://doi.org/10.21203/rs.3.rs-3518210/v1

Additional Declarations: No competing interests reported.

Version of Record: A version of this preprint was published at Biomechanics and Modeling in Mechanobiology on March 28th, 2024. See the published version at https://doi.org/10.1007/s10237-024-01828-4.

Preliminary establishment and validation of the inversion method for growth and remodeling parameters of patient-specific abdominal aortic aneurysms.

Chen Peng[1, 5†], Wei He[2†], Jingyang Luan[2], Tong Yuan[2], Weiguo Fu[2,3,4], Yun Shi[2,3,4*], Shengzhang Wang[5,6,7*]

[1]Artificial Intelligence Research Institute, Zhejiang Lab, Hangzhou, Zhejiang, China.

[2]Department of Vascular Surgery, Zhongshan Hospital, Fudan University, Shanghai, China,

[3]Institute of Vascular Surgery, Fudan University, Shanghai, China,

[4]National Clinical Research Center for Interventional Medicine, Fudan University, Shanghai, China,

[5]Department of Aeronautics and Astronautics, Institute of Biomechanics, Fudan University, Shanghai, China

[6]Institute of Biomedical Engineering Technology, Academy for Engineering and Technology, Fudan University, Shanghai, China,

[7]Yiwu Research Institute, Fudan University, Yiwu, Zhejiang, China.

* CORRESPONDENCE

Yun Shi, shi.yun@zs-hospital.sh.cn

Shengzhang Wang, szwang@fudan.edu.cn

† These authors have contributed equally to this work

Abstract

Background: Traditional medical imaging studies and biomechanical researches have limitations in analyzing the long-term evolution process of AAA (Abdominal Aortic Aneurysm, AAA). The HCMT (Homogenized Constrained Mixture Theory, HCMT) allows for quantitative analysis of the changes of the three-dimensional morphology and composition of AAA. However, the accuracy of HCMT still requires further clinical verification.

Objective: This study aims to establish a patient-specific AAA growth model based on HCMT, simulate the long-term G&R (Growth and Remodeling G&R) process of AAA, and validate the feasibility and accuracy of the method using two additional AAA cases with 5 follow-up data.

Methods: The media and adventitia of the aorta were modeled as mixtures composed of elastin, collagen fibers, and SMC (smooth muscle cells, SMC). The strain energy function was used to describe the continuously generation and degradation of the mixture during the AAA G&R process. Multiple sets of growth parameters were applied to finite element simulations, and the simulation results were compared with the follow-up data for gradually selecting the optimal growth parameters. Two additional AAA patients with different growth rates were used for validating the method, the optimal growth parameters were obtained using the first two follow-up imaging data, and the growth model was applied to simulate the subsequent four time points. The differences between the simulated diameters and the follow-up diameters of AAA were compared to validate the accuracy of the growth model.

Results: The growth parameters, especially the stress-mediated substance deposition gain factor K_{σ}^{i}, is highly related to the AAA G&R process. When setting the optimal growth parameters to simulate AAA growth, the proportion of simulation results within the distance of less than 0.5 mm from the follow-up model is above 80%. For the validating cases, during the 5 follow-up processes, the mean difference rates between the simulated diameter and the real-world diameter are within 2.5%, which basically meets the clinical demand for quantitatively predicting the AAA growth in maximum diameters.

Conclusion: This study simulated the growth process of AAA, and validated the accuracy of this growth model. This method was proved to be used to predict the G&R

process of AAA caused by dynamic changes in the mixtures of the AAA vessel wall at a long-term time scale, assisting accurately and quantitatively predicting the multi-dimensional morphological development and mixtures evolution process of AAA in clinic.

Keywords: Abdominal Aortic Aneurysms; Growth and Remodeling; Homogenized Constrained Mixture Theory; Inverse Method; Finite Element Simulation.

Introduction

In the preoperative diagnosis of AAA (Abdominal Aortic Aneurysm, AAA) detected through early medical imaging techniques, clinical recommendations indicate that patients with a maximum AAA diameter reaching 55 mm are at high risk of rupture and require prompt surgical intervention[1]. When it comes to preoperative diagnosis of AAA detected through medical imaging techniques, it is important to note that the maximum diameter only describes the current state of AAA, disregarding the developmental process. Researches conducted by both domestic and international scholars has revealed that some AAA may rapid growth and rupture even when they have not reached the diameter threshold. Conversely, AAA with a maximum diameter exceeding 55mm can remain stable over a long period of time[2,3]. Therefore, the challenge currently faced in the field of preoperative diagnosis of AAA is how to quantitatively assess the long-term development process of AAA in multi-dimension.

Traditional bio-mechanical computational methods, such as finite element simulations that consider factors like stress and strain of vessel wall, computational fluid dynamics simulations that analyze parameters like intra-vascular flow patterns and pressure, fluid-structure interaction simulations that simultaneously account for the interaction between blood and vessel wall, have been widely applied in the preoperative diagnosis of AAA[4–6]. However, most of these studies primarily qualitatively assessed the growth or rupture tendencies of AAA based on transient imaging data. They overlook the morphological development and material evolution processes of patient-specific AAA over a long-term scale. As a result, their clinical applicability has been limited in terms of providing valuable references.

Theoretical models of the G&R (Growth and Remodeling, G&R) can quantitatively analyze the changes in the morphology and composition of soft tissues,

thus enhancing our understanding of the long-term development of vascular diseases. The mechanical model based on the CMT (Constrained Mixture Theory, CMT) considers physiological processes such as degradation, deposition, and remodeling of different components of the vessel wall[7]. Watton et al. simplified AAA as an ideal cylindrical model but did not investigate the growth process of patient-specific AAAs[8,9]. Some researchers have also used one-way FSI simulations to capture the dynamic evolution of the vessel wall, considering the stimulating effect of wall shear stress on the degradation of elastin in AAA growth process and further investigated the dynamic changes in growth parameters. However, the mechanical model became overly complex and difficult to operate[10,11]. To address the issue of timeliness, Do et al., using longitudinal CTA (Computational Tomography Angiography, CTA) scans and the DGPIS (Dynamical Gaussian Process Implicit Surface, DGPIS) to predict AAA growth in a patient-specific way[12]. Jiang et al., combined AAA G&R model and deep learning method which can provide deterministic patient-specific predictions of AAA expansion[13]. Nevertheless, when simulating over a long period of time, there are significant discrepancies between the simulation results and the corresponding results from the follow-up image data.

Although the aforementioned studies were capable of simulating aneurysm growth, they commonly suffered from deficiencies such as lack patient specificity due to excessive model simplification[14,15], without validation through in vitro experiments or multiple follow-up image data[16], insufficient computational efficiency, and difficulty in practical application to clinical problems[17].

In this study, the HCMT (Homogenized Constrained Mixing Theory, HCMT) was used to simulate the growth process of early-stage AAA, and different sets of growth parameters were adjusted. The simulation results could subsequently be matched with the geometric model reconstructed from follow-up CTA data at the corresponding time, to obtain the optimal growth parameters. After the initial establishment of the growth model, the accuracy of the growth model was validated by two additional AAA cases of different growth rates with 5 follow-up CTA data.

2 Method

2.1 Data acquisition

This study established the growth model using AAA CTA data with two follow-up time points. Additionally, two cases with five follow-up image data were used to validate the accuracy of the method during longer period of time, as shown in Table 1. The CTA image data collected in this study was approved by the Ethics Committee of Zhongshan Hospital, Fudan University and informed consent forms were waived due to the retrospective study.

Table 1: Summary of subject demographics.

	Gender	Age	Scan times	Time interval(months)	Maximum diameter(mm)
Case 1	Male	76	2	39	15.33, 24.95
Case 2	Female	69	5	6, 12, 7, 5	14.52, 15.67, 17.74, 18.91, 20.27
Case 3	Male	69	5	36, 24, 12, 12	15.15, 17.13, 18.45, 19.19, 20.41

2.2 Model reconstruction

To avoid the errors caused by manual segmentation, we utilize an AI-based automatic segmentation algorithm based on U-NET to suppress information such as bones and organs, retaining only the image information related to the aorta[18]. Then, the models were imported into Geomagic Studio for smoothing and trimming, resulting in the geometric model of the region of interest. As the morphological development process of AAA is of greater clinical concern, we specifically removed the distal iliac arterial branches and the proximal aorta, retained only the aneurysm, and generated NURBS surfaces, the process was shown in Figure 1.

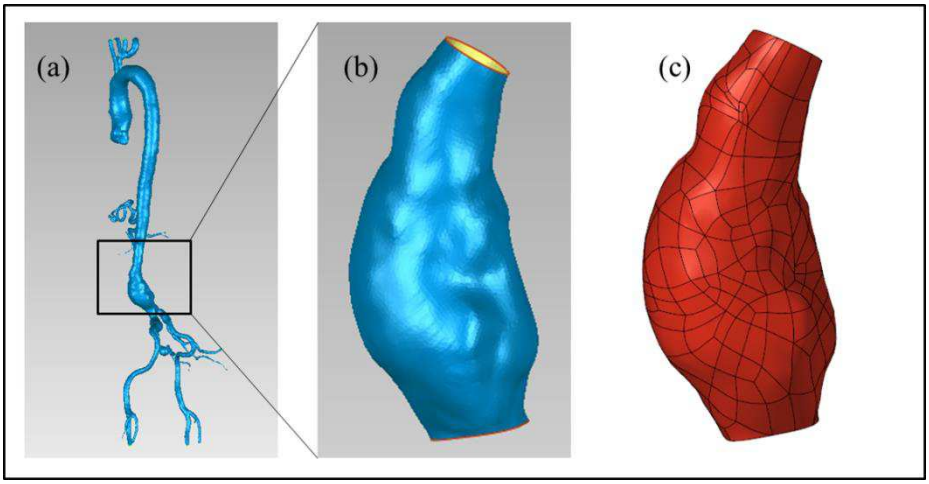

Fig. 1. Geometric model reconstruction process (a) Aorta geometric reconstruction. (b) Smooth and segmentation of the AAA. (c) NURBS surface generation.

2.3 The establishment of patient-specific AAA growth and remodeling models.

2.3.1 Extraction of centerline.

To minimize measurement errors in obtaining the maximum diameter of AAA due to differences in planes, measurement axes, angles, and operators, the researchers in this study used the open-source software VMTK to extract the centerline of the geometric model and the variation of the maximum inscribed sphere radius along the centerline[19], the specific method is as follows:

Step 1: Suppose there is a sphere located inside the blood vessel, tangent to the aorta. The center of this sphere is defined as a point of the aorta centerline.

Step 2: The sphere moves within the aorta while remaining tangent to the vessel wall. The radius of the sphere changes, and the line connecting the centers corresponding to different spheres is defined as the centerline, as shown in Figure 2(a).

Step 3: The radius variations along the centerline of AAA are obtained, as shown in Figure 2(b).

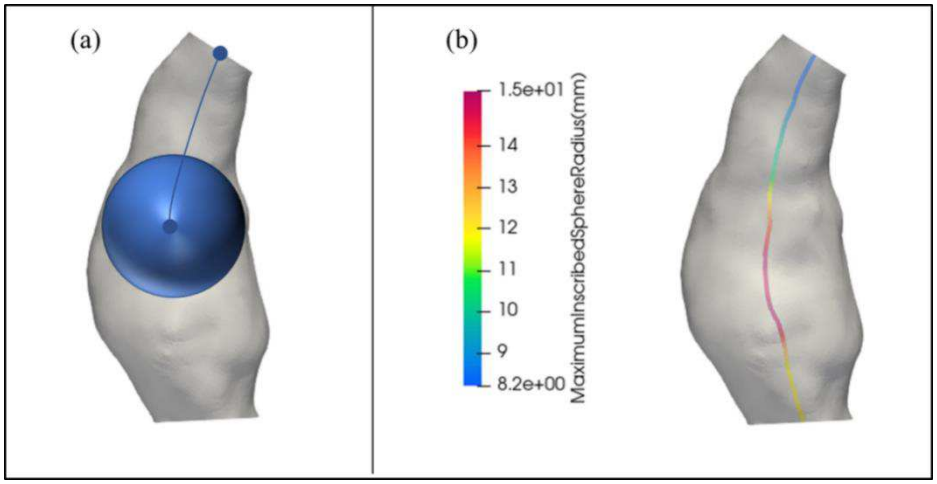

Fig. 2. Extraction of the centerline. (b) The maximum diameter of the inscribed sphere along the centerline.

2.3.2 Mesh generation

The NURBS surface corresponding to the AAA model is imported into Hypermesh for structured mesh generation, as shown in Figure 3(a). Based on the measured experimental data (**Supplementary material: Module 1**), the shell elements were offset outward by 2.27mm to represent the thickness of the aorta. The generated solid elements were shown in Figure 3(b). The solid elements were then divided into media and adventitia layers (For the reason that the intima layer is very thin and plays a minor role in the solid mechanical properties of the aorta[20], as shown in Figure 3(c).

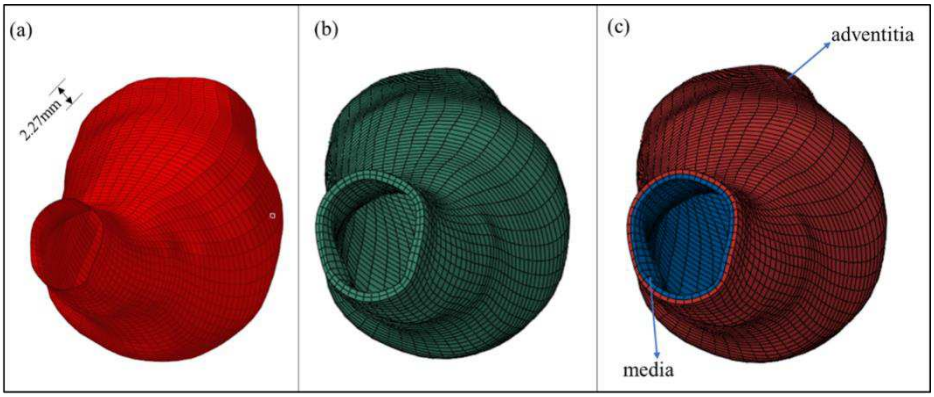

Fig. 3. The process of mesh generation. (a) Surface mesh generation. (b) Offset of the structured mesh to obtain solid mesh. (c) Elements Divided into media and adventitia layers.

2.3.3 Definition of local coordinate system

The arrangement direction of collagen fibers and smooth muscle fibers in HCMT is defined based on the angle with respect to the circumferential direction of the blood

vessel wall as mentioned in the supplementary material. Therefore, in order to capture the fiber orientation at different locations of the vessel wall, it is necessary to define a local coordinate system for each element, the specific method is as follows:

Step 1: Import the centerline into the model as a reference line for generating the local coordinate system, as shown in Figure 4(a)[21,22].

Step 2: Consider the outward normal direction perpendicular to the outer surface of the blood vessel wall as the radial direction, the direction parallel to the centerline as the axial direction, and the circumferential direction as the cross product of the axial and radial directions, as shown in Figure 4(b).

Step 3: The local magnification effect of the local coordinate system is shown in Figure 4(c).

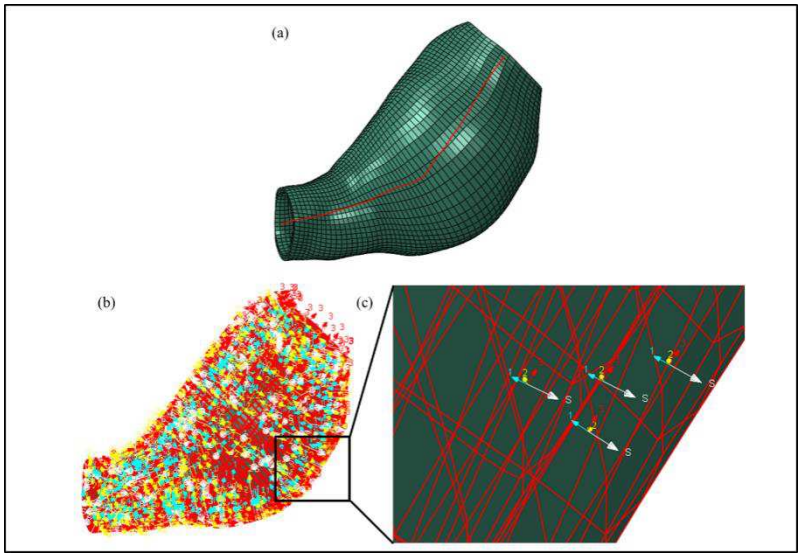

Fig. 4. Creation of local coordinate system. (a) Importing the centerline into the finite element model. (b) Creating local coordinate systems on each element. (c) Local magnification diagram.

2.3.4 Mass density distribution and material parameters at the initial moment.

Each unit volume of the middle layer and adventitia layer of the aorta was considered a mixture composed of elastin, four clusters of collagen fibers, and one cluster of smooth muscle fibers. The mass densities of these six components in each layer are different according to reference, as shown in Table 2[23]. The partial material parameters of different components are shown in Table 3.

Table 2: Mass density distribution of different tissue components.

	Elastin(kg/m^3)	Collagen(kg/m^3)			SMC(kg/m^3)
		circumferential	axial	diagonal	
Media	169	14.6	48.5	58.4	735
Adventitia	565	14.6	48.5	194	0
Sum	734	29.2	97	252.4	735

Table 3: Material parameter Settings at the initial moment of G&R process

Symbols	**value**
$\alpha^{c_j}, j = 1,2,3,4$	$\frac{\pi}{2}, \frac{\pi}{4}, \frac{\pi}{4}, 0$
μ^e	82(J/kg)
κ	8200(J/kg)
$k_1^{c_j}$	15(J/kg)
$k_2^{c_j}$	1.0
k_1^m	10(J/kg)
k_2^m	0.1
λ_z^e	1.3
λ^{c_j}	1.1
λ^{smc}	1.1
λ_{smc}^0	0.8
T^e	101(years)
T^{c_j}	101(days)
T^m	101(days)
σ_{actmax}^{smc}	54 KPa

2.3.5 Boundary conditions and load conditions.

The axial and circumferential directions were fixed at the aortic inlet and outlet to ensure the grid nodes move only circumstantially[22].

The intro-vascular load is set to $\frac{1}{3}(P_s + 2P_d)$, where P_s and P_d are systolic blood pressure and diastolic blood pressure, respectively. Based on the medical history

information, the pressure of the three cases was set to 91 mmHg, 103 mmHg and 87 mmHg, respectively.

2.3.6 Strain energy function definition

The application of HCMT in ideal thick-wall tube has been introduced in detail from **Module 2 to Module 4 of the supplementary materials**. The form of Cauchy stress matrix and stiffness matrix can be seen in equation (s31) and equation (s32) of the **supplementary material: Module 5**, the specific derivation process will not be repeated.

It is worth noting that due to the irregular shape of aneurysms, it is not possible to define that the degradation of elastin occurs at its fastest rate in the middle of an ideal circular tube and gradually decreases as it approaches the ends of the tube[22]. Therefore, we need to define an alternative function to describe the degradation process of elastin.

The development of AAA is accompanied by the spatially unevenly distributed degradation of elastin, which may be related to high wall stress at the location of the aneurysm formation[24].We assumed that when a point on the aorta is farther away from the center line, the degradation rate of elastin is faster, and vice versa, the degradation rate of elastin is slower. We define an exponential function to describe the evolution of elastin over time and space, as shown in equation (1):

$$\dot{D}_g^e(\boldsymbol{X},t) = -\frac{\rho^e(\boldsymbol{X},t)}{T^e} - \frac{D_{max}}{t_{dam}}\rho^e(\boldsymbol{X},0)e^{-0.5\left(\frac{\min|\mathbf{X}_d|}{R_m}\right)^2} e^{-\frac{t}{t_{dam}}} \quad (1)$$

where $\min|\mathbf{X}_d|$ represents the minimum distance from the center coordinates of one specific element to the centerline of AAA, R_m representing the maximum diameter of AAA.

Under the aforementioned conditions, the strain energy function evolving in time and space can be constructed using UMAT to describe the dynamic variations of the constitutive model in the G&R process, caused by degradation, remodeling, and deposition of the mixture.

2.3.7 Stepwise screening of growth parameters.

In the **supplementary materials: Module 6**, the effects of variations in three parameters, including the K_σ^i (gain factor of stress-mediated fibers deposition), t_{dam}(the time diffusion factor of elastin damage), and λ_{actmax}^{smc} (the maximum active

stretch of SMCs), on the G&R process were analyzed. K_{σ}^{i} mainly affects the morphological development and collagen fibers evolution process of AAA, while the changes of t_{dam} and λ_{actmax}^{smc} have little influence on the morphology of aneurysms, but can affect variables such as thickness, collagen fiber deposition and active smooth muscle stretching.

Inspired by the approach of obtaining the optimal material parameters through a step-by-step screening process in our previous article[25], in this study, a set of 14 values for parameter K_{σ}^{i}, as well as three sets of values for parameters t_{dam} and λ_{actmax}^{smc}, were selected as the candidate growth parameter sets. This selection aimed to ensure that the local optimal solutions for the growth parameters lie within the range of the parameter combinations being screened, as shown in Table 4.

Table 4: Candidate growth parameter sets for AAA in the G&R process

Growth parameters	K_{σ}^{i}	t_{dam}	λ_{actmax}^{smc}
values	[0.03,0.16]/T_{C_i} Increment:0.01	20 days, 40 days, 80 days.	1.4, 1.5, 1.6

Considering that K_{σ}^{i} plays a significant role in the G&R process of AAA(as shown in **Module 6 of supplementary material**), the study first aims to determine the corresponding value of K_{σ}^{i} for each individual case. The specific process involves as follows:

Step 1: Substituted the value of K_{σ}^{i} into the growth model and arbitrarily selected a set of values for t_{dam} and λ_{actmax}^{smc} to simulate the G&R process of AAA. Paused the finite element simulation when the simulated time aligns with the interval between two follow-up data points.

Step 2: Extracted the geometric information of the inner surface of the AAA vessel wall after simulation and compared it with the model reconstructed based on follow-up data, and record the distance.

Step 3: Selected different values of K_{σ}^{i} and repeat the first two steps. Obtained the optimal solution when the distance between the simulation results and the model reconstructed based on follow-up data is minimized.

Step 4: Used the remaining 8 sets of t_{dam} and λ_{actmax}^{smc} to adjust the G&R process of AAA using the growth model. Similarly, used the distance between the simulated model and model reconstructed based on follow-up data as a reference. When the

distance is minimized, considered the combination of the three growth parameters as the corresponding optimal solution in Table 4.

2.4 Accuracy validation of AAA growth and remodeling model

After the preliminary establishment of the growth model, it is necessary to validate its accuracy by applying it to the patient-specific G&R process of AAA. The specific operational process is as follows:

Step 1: Build the growth model using the follow-up data from the first two time points and obtain an optimal set of growth parameters using the method described in section 2.3.

Step 2: Keep the growth parameters consistent and continue the simulation of the G&R process for AAA at the subsequent follow-up time point. Compare the simulation results at different follow-up time points with the follow-up results.

Step 3: Validate the accuracy of the growth model using different morphological parameters. Parameter 1: Radius variation along the centerline. Parameter 2: Maximum radius of AAA at different follow-up time points.

3 Results

3.1 Comparison of Simulation Results and Follow-up Data

The inversion of growth parameters for the AAA model involving two time points in the method yielded a set of optimal solutions for K_{σ}^{i}, t_{dam} and λ_{actmax}^{smc}, which were determined to be $\frac{0.06}{101\mathrm{days}}$, 40days and 1.5, respectively. The distribution of distances between the inner surface of the vessel wall obtained from the simulation results and the model reconstructed based on follow-up data from the second time point is shown in Figure 5(a), while the matching results of the model are shown in Figure .5(b).

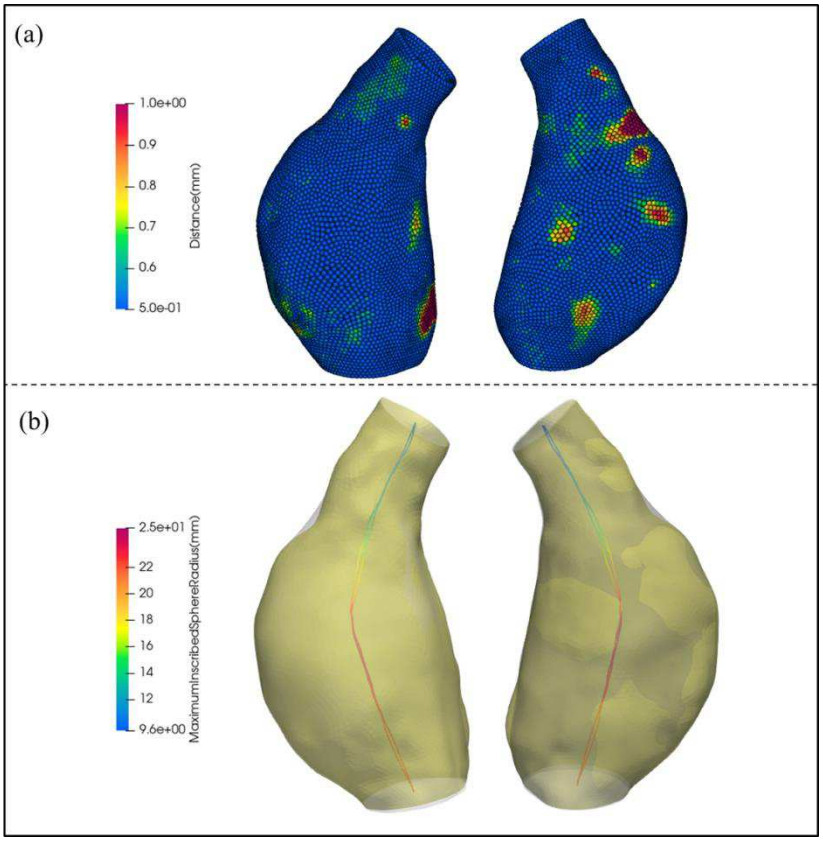

Fig. 5. (a) The distribution of distances between the simulated results and the reconstructed model based on follow-up data. (b) The matching results of the two models.

When the distance between the simulated results and the follow-up data nodes is less than 0.5 mm (the typical resolution of CT scans), it is considered to have a high degree of matching. Calculations reveal that the proportion of distances less than 0.5mm is 82.05%. The distance significantly increases in the proximal neck and the region near the posterior aspect in the distal of the AAA. The maximum radius variation along the centerline corresponding to the simulated results and the model reconstructed from the second follow-up data is depicted in Figure 5 (b). By comparing it with Figure 2 (b), it can be observed that the upper end of AAA, which did not undergo expansion in the simulation process, shows little change in radius, only increasing by 1.3 mm. However, the maximum radius increases from 15.1 mm to 25.20 mm, indicating significant differences in the growth rate of the aneurysm at different positions of the AAA vessel wall.

The model reconstructed from follow-up data exhibits significant shrinkage (highlighted in yellow) at the proximal neck, while no similar phenomenon was observed during the simulation of the G&R process for AAA (shown as semi-transparent). Additionally, in the distal of the AAA near the posterior aspect, there is

noticeable expansion in the simulated results, whereas the model reconstructed based on imaging data does not show expansion.

Furthermore, in Figure 5 (b), it can be observed that the simulated results and the model reconstructed based on follow-up data have almost identical positions along the centerline. Next, in order to compare the clinically relevant AAA diameter information, the study utilized the method mentioned in section 2.3.1 to extract the radius of the centerline, as shown in Figure 6.

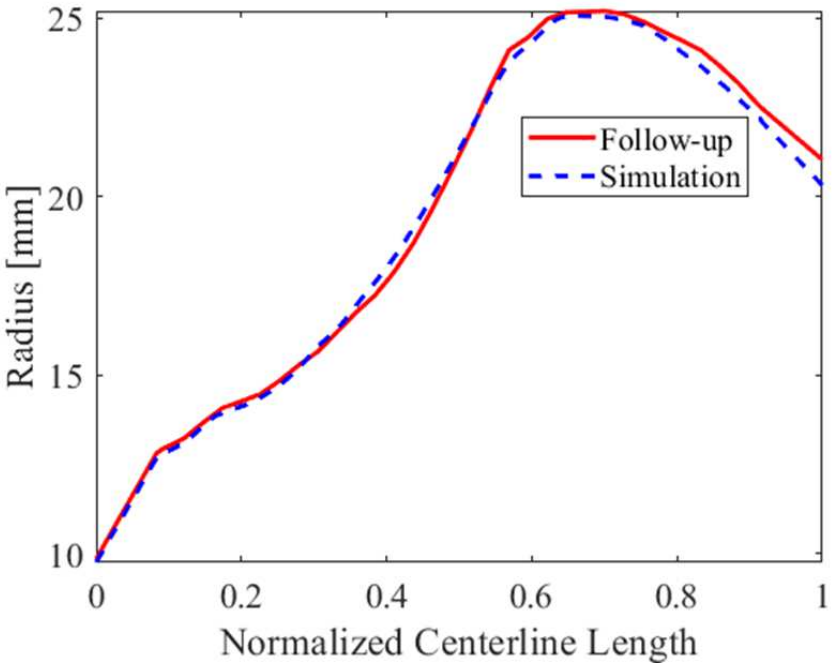

Fig.6. The variation of the radius along the centerline of the models reconstructed based on follow-up data and the simulated results.

It can be observed that along the normalized centerline length, the curves of the maximum inscribed sphere radius for both models almost overlap, with an R^2 value of 0.9787, indicating a high degree of matching. The maximum diameter of the simulated results is 25.07mm, with a difference of 0.52% compared to the maximum diameter corresponding to the follow-up data.

3.2 Accuracy validation of AAA growth model.

Next, two additional AAA cases with 5 follow-up data were selected (see Table 1) to validate the accuracy of the growth parameter inversion method based on the first two time points of the follow-up data.

After completing the mesh generation and finite element solution setup, according

to the method of inverting growth parameters, the optimal solutions for the growth parameters of these two cases can be obtained based on the follow-up data of the first two time points of the AAA patients, which are {0.08/101 days, 40 days, 1.5} and {0.16/101 days, 20 days, 1.4}, respectively.

The diameters along the centerline of the geometric models created at different time points based on the follow-up data were extracted and compared with the diameters along the centerline of the geometric models simulated at corresponding time points. The results are shown in Figure 7.

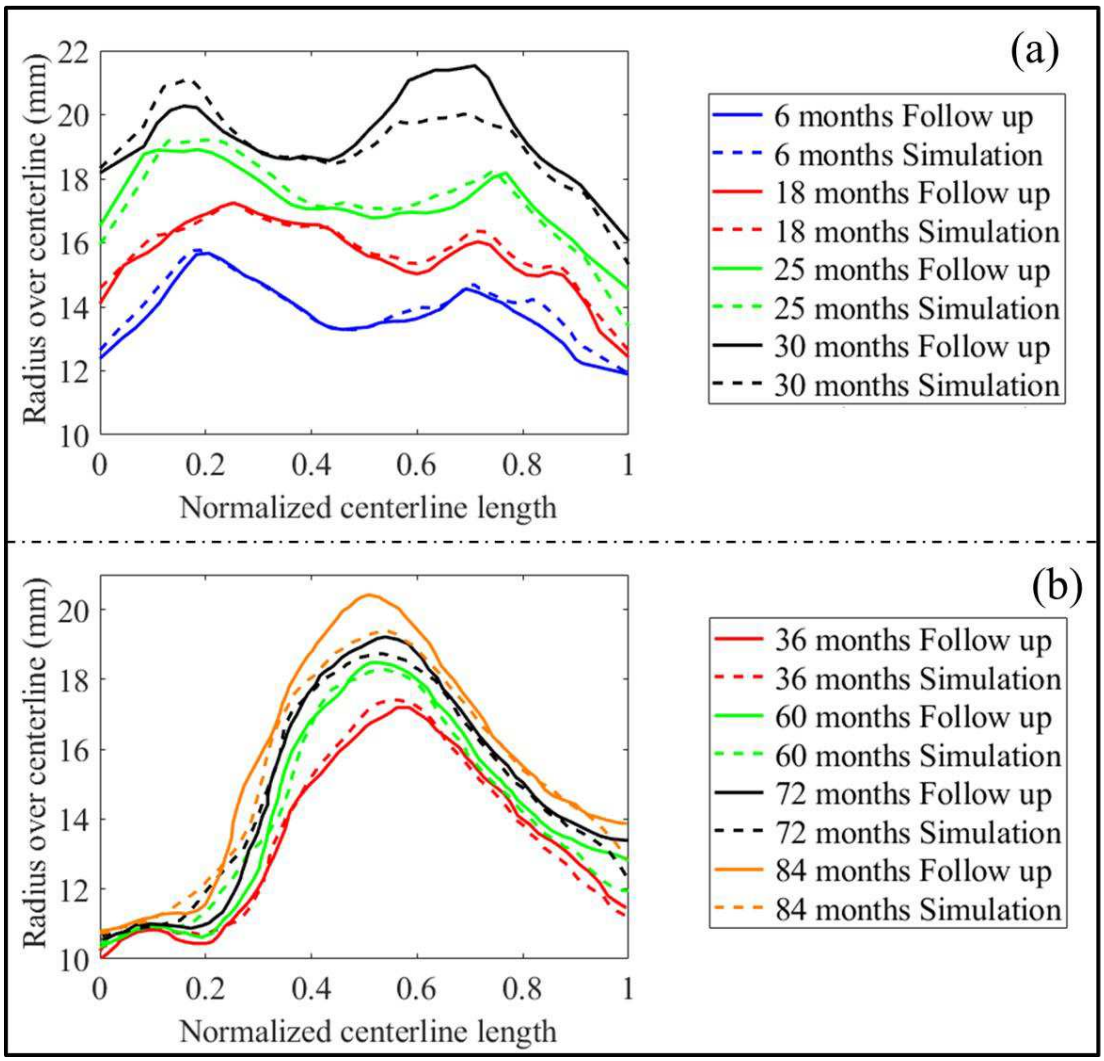

Fig.7. The variation of the radius along the centerline of the models reconstructed based on follow-up data and the models obtained from simulation at different time points for (a) Case 2 and (b) Case 3.

It can be observed that, for Case 1, the real-world models and the simulated models have consistent trends in terms of the radius variation along the centerline at the first three follow-up time points. When the simulation time reaches 30 months, the expansion of the abdominal aortic aneurysm (AAA) downstream is smaller, and its

diameter remains smaller than that of the upstream aneurysm. In contrast, based on the radius variation information reflected by the follow-up data, from the 25th month to the 30th month, the change in radius for the upstream aneurysm is relatively small, increasing from 18.91mm to 20.27mm. On the other hand, the downstream aneurysm radius increases from 17.73mm to 21.68mm. The growth trend of the abdominal aorta undergoes a significant change in a short period of time, and the maximum radius of the downstream AAA exceeds that of the upstream AAA.

For Case 2, at the four follow-up time points, the radius variation along the centerline obtained showed consistent trends. There is no significant change in the radius at the upstream of the aneurysm neck near the proximal abdominal aorta and the downstream of the aneurysm neck near the distal abdominal aorta. The maximum diameter increases by 6.56mm over a 4-year period from the second to the fourth scan time point, indicating that the aneurysm remains relatively stable. It is worth noting that the optimal solution for $K_{\sigma}^{i} = 0.16/101$ days, indicating a relatively fast deposition rate of collagen fibers. This compensates for the stress that cannot be supported due to the degradation of elastin. The simulation results show that there is no significant change in the maximum diameter of the AAA between the 6th and 7th year. However, the maximum diameter reflected by the follow-up data in this year shows a relatively significant change, possibly due to sudden physiological changes.

In clinical, the maximum diameter of the AAA remains the gold standard for determining whether to perform surgical intervention on patients. For both cases, we compared the maximum diameters at the 2nd to 5th follow-up time points (based on the first aneurysm appearance from the proximal to the distal end), as summarized in Table 5.

Table 5: The comparison of the maximum AAA diameter corresponding to the follow-up data and the simulation results.

	Maximum diameter comparison	Case1	Case2
The second follow up	Maximum diameter (follow up) (mm)	31.34	34.26
	Maximum diameter (simulated) (mm)	31.54	34.80
	Relative error (%)	0.64	1.58
The third follow up	Maximum diameter (follow up) (mm)	35.48	36.90
	Maximum diameter (simulated) (mm)	34.48	36.56
	Relative error (%)	2.82	0.92
The fourth follow up	Maximum diameter (follow up) (mm)	37.82	38.38
	Maximum diameter (simulated) (mm)	38.42	37.66
	Relative error (%)	1.59	1.88
The fifth follow up	Maximum diameter (follow up) (mm)	40.54	40.82
	Maximum diameter (simulated) (mm)	42.22	38.82
	Relative error (%)	4.14	4.90
	Annual average relative error. (%)	2.07	1.23

For two cases with different growth rates of AAA, the error between the maximum diameter obtained from simulation at four specific time points and the maximum diameter obtained based on follow-up data does not exceed 5%. The annual average error of the maximum diameter for case 1 over the next two years is 2.07%, and for case 2 over the next 4 years is 1.23%. This can effectively meet the clinical demand for quantitatively predicting the trend of maximum diameter changes of AAA.

4 Discussion

There is still no comprehensive theory that can quantitatively analyze the morphological development and material evolution process of AAA on a large time scale accurately. The change rate of the AAA maximum diameter based on follow-up imaging data can only provide information in a single dimension and cannot predict the

morphological development of AAA in multiple dimensions[26,27]. Commonly used bio-mechanical computational models couple imaging data from a single time point with numerical simulation methods to qualitatively assess the trend of AAA growth or rupture[28,29], overlooking the long-term development process of AAA. Recently, Some have also attempted to use artificial intelligence methods to predict the growth of aneurysms, but models are lack the implementation of fundamental bio-mechanical laws[30,31].

This study is based on the HCMT theory and simulates the growth process of patient-specific AAA on a large time scale. Firstly, several sets of growth parameters are created, and the optimal growth parameters of different AAA is determined using follow-up data from the first two time points. Next, the accuracy of the growth parameter inversion method is validated using AAA cases with multiple follow-up time points. The aforementioned method can effectively predict the G&R process of patient-specific AAA, providing a reference for quantitatively predicting the multidimensional morphological development and material evolution of early AAA cases in clinical practice.

In addition to predicting morphological changes, this study also analyzed the substance and wall thickness variations of AAA with different growth rates, as shown in Figure 8.

For case 1, which has a faster growth rate, the optimal solution for the K_{σ}^{i} value is 0.08/(101 days). Rapid degradation of elastin near the maximum diameter, leading to an increasing stress on the AAA vascular wall[22]. Consequently, under the influence of stress, collagen fibers continue to be rapid deposited to compensate for the loss of elastin and maintain the vascular wall's stability under physiological pressure. Over the course of three years, the collagen fiber deposition in case 1 is 2.4 times that of the initial stage. In contrast, for case 2 with a slower AAA growth rate, significant collagen fiber deposition is not necessary to maintain the stability of the vascular wall. The collagen fiber deposition is only 1.1 times that of the initial stage, indicating a significant difference between these two cases.

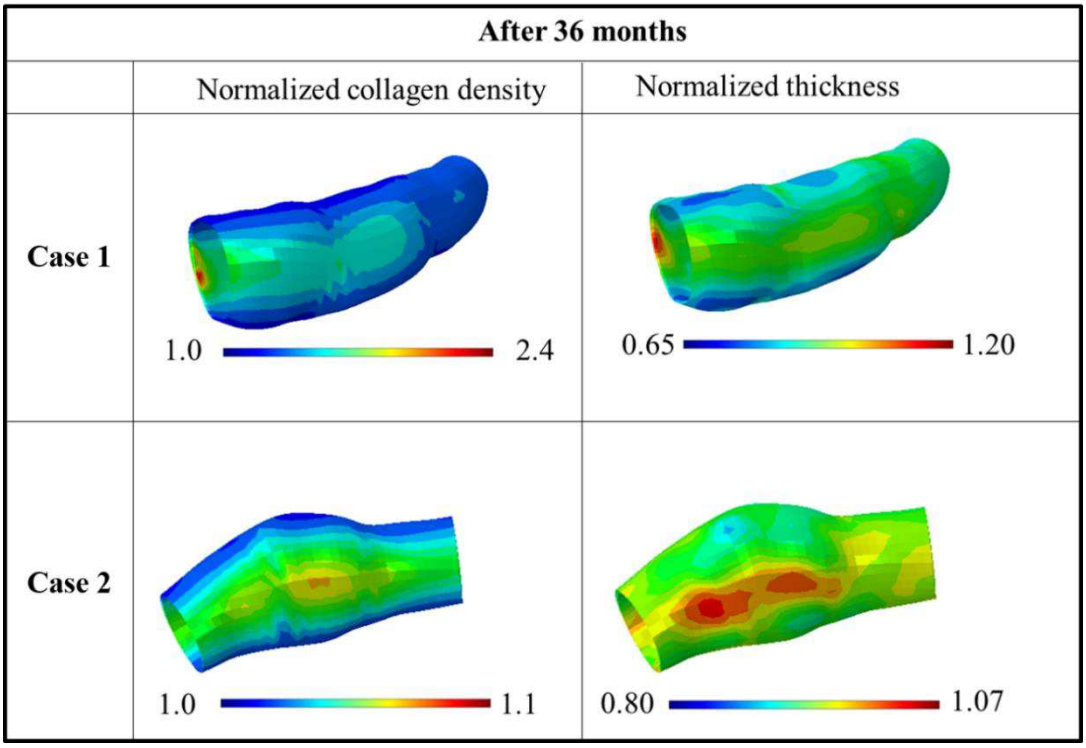

Fig.8. After 36 months of simulation, the standardized distribution of collagen fiber density and vascular wall thickness was analyzed for case 2 and case 3.

Additionally, collagen fibers tend to deposit in areas where elastin degrade most rapidly, resulting in an increase in vascular wall thickness, which can lead to arterial wall stiffening[32]. In regions where there is no turnover of collagen fiber production, the thickness of the vascular wall is reduced. In the two cases, the thickness near the region with the highest relative density of collagen fibers is 1.2 times and 1.07 times that of the initial thickness, respectively. Dar Weiss et al., found that aneurysm dilatation correlating with compromised elastic fiber integrity and rupture correlating with compromised collagen fibril organization[33]. Our research warrants further refinement through the execution of in vitro experiments to elucidate the dynamic alterations in collagen fiber density and vascular wall thickness throughout the progression of AAA, which will allow us to further validate the accuracy of the growth model at the microscopic histological level.

As AAA continues to grow, the differences in the maximum diameter and the diameter changes along the centerline corresponding to the simulation results and the follow-up data become increasingly apparent. In Figures 5, the simulated AAA expands towards the back side, while the reconstructed AAA based on imaging data does not

exhibit this phenomenon. This may be due to the fact that this study did not consider the constraining effect of the spine on AAA growth, causing the aneurysm to expand towards the back side. In actual physiological conditions, most AAAs are constrained by the spine during the growth process[34], resulting in less expansion towards the back side and more expansion towards the abdominal side. This deviation from real-life conditions leads to discrepancies between simulation results and actual situations. In the actual follow-up process, the overall asymmetry of AAA (the definition of asymmetry can be seen in[35]. shows a gradually increasing trend, while the corresponding asymmetry of the simulated results decreases gradually[36]. These results also indicate the importance of considering the constraining effect of the spine on AAA[37].

During the development of AAA, there are associated changes in the physiological environment. For instance, the formation and progression of mural thrombus can impact the hemodynamic environment and the material evolution of the vessel wall[38,39]. Quantifying the development process of thrombus, especially the release of proteinase molecules associated with the structural stratification of the clot, which may affect localized weakening of the aneurysm wall[40]. Additionally, the deposition of collagen fibers under stress-mediated conditions, turnover rate of different tissues, the extent of strain under steady state, as manifested in growth parameters, are also likely to change during the process of AAA occurrence and progression[16,41]. Subsequent studies should consider the dynamic changes in biochemical and mechanical factors during the G&R process of AAA.

5 Conclusion

This study established one patient-specific growth model based on the HCMT to simulate the long-term G&R process of early-stage AAA. The accuracy of the growth model was validated using follow-up data at multiple time points. At different follow-up time points, the trends of diameter changes along the AAA centerline obtained from

simulation results and follow-up data were consistent, with differences in maximum AAA diameter not exceeding 3%. This study provides a preliminary approach to simulate the long-term growth process of early-stage AAA based on CTA and bio-mechanical models. The growth model for simulating patient-specific AAA G&R process holds promise to accurately and quantitatively predict the multidimensional morphological development and material evolution processes of AAA, distinguish AAA with different growth rates, and provide appropriate surgical plans for patients in clinic.

Declaration of competing interest

The authors declare that they have no known competing financial interests or personal relationships that could have appeared to influence the work reported in this paper.

Acknowledgments

This study was supported by the National Natural Science Foundation of China (No. 11872152, 32071310, 81770508).

Reference

[1] Grima M J, Behrendt C A, Vidal-Diez A, et al. Editor's Choice – Assessment of Correlation Between Mean Size of Infrarenal Abdominal Aortic Aneurysm at Time of Intact Repair Against Repair and Rupture Rate in Nine Countries[J/OL]. European Journal of Vascular and Endovascular Surgery, 2020, 59(6): 890-897. DOI:10.1016/j.ejvs.2020.01.024.

[2] Qiu Y, Wang J, Zhao J, et al. Association Between Blood Flow Pattern and Rupture Risk of Abdominal Aortic Aneurysm Based on Computational Fluid Dynamics[J/OL]. European Journal of Vascular and Endovascular Surgery, 2022, 64(2-3): 155-164. DOI:10.1016/j.ejvs.2022.05.027.

[3] Joly F, Soulez G, Lessard S, et al. A Cohort Longitudinal Study Identifies Morphology and Hemodynamics Predictors of Abdominal Aortic Aneurysm Growth[J/OL]. Ann

als of Biomedical Engineering, 2020, 48(2): 606-623. DOI:10.1007/s10439-019-02375-1.

[4] Canchi T, Saxena A, Ng E, et al. Application of Fluid–Structure Interaction Methods to Estimate the Mechanics of Rupture in Asian Abdominal Aortic Aneurysms[J/OL]. BioNanoScience, 2018, 8(4): 1035-1044. DOI:10.1007/s12668-018-0554-z.

[5] Silva J L, Belinha J, Neves J M P R, et al. Numerical simulation of aneurysms wit h Finite Element and Meshless Methods[C/OL]//2019 IEEE 6th Portuguese Meeting o n Bioengineering (ENBENG). 2019: 1-4. DOI:10.1109/ENBENG.2019.8692459.

[6] Algabri Y A, Chatpun S, Taib I. An Investigation of Pulsatile Blood Flow in An A ngulated Neck of Abdominal Aortic Aneurysm Using Computational Fluid Dynamics[J]. Journal of Advanced Research in Fluid Mechanics and Thermal Sciences, 2019, 5 7(2): 265-274.

[7] Humphrey J D, Rajagopal K R. A CONSTRAINED MIXTURE MODEL FOR GRO WTH AND REMODELING OF SOFT TISSUES[J/OL]. Mathematical Models and M ethods in Applied Sciences, 2002, 12(03): 407-430. DOI:10.1142/S0218202502001714.

[8] Watton P N, Hill N A, Heil M. A mathematical model for the growth of the abdom inal aortic aneurysm[J/OL]. Biomechanics and Modeling in Mechanobiology, 2004, 3(2): 98-113. DOI:10.1007/s10237-004-0052-9.

[9] Watton P N, Hill N A. Evolving mechanical properties of a model of abdominal aor tic aneurysm[J/OL]. Biomechanics and Modeling in Mechanobiology, 2009, 8(1): 25-4 2. DOI:10.1007/s10237-007-0115-9.

[10] Sheidaei A, Hunley S C, Zeinali-Davarani S, et al. Simulation of abdominal aortic a neurysm growth with updating hemodynamic loads using a realistic geometry[J/OL]. Medical Engineering & Physics, 2011, 33(1): 80-88. DOI:10.1016/j.medengphy.2010.0 9.012.

[11] Grytsan A, Watton P N, Holzapfel G A. A Thick-Walled Fluid–Solid-Growth Model of Abdominal Aortic Aneurysm Evolution: Application to a Patient-Specific Geometry [J/OL]. Journal of Biomechanical Engineering, 2015, 137(3): 031008. DOI:10.1115/1.4 029279.

[12] Do H N, Ijaz A, Gharahi H, et al. Prediction of Abdominal Aortic Aneurysm Growt h Using Dynamical Gaussian Process Implicit Surface[J/OL]. IEEE Transactions on B iomedical Engineering, 2019, 66(3): 609-622. DOI:10.1109/TBME.2018.2852306.

[13] Jiang Z, Do H N, Choi J, et al. A Deep Learning Approach to Predict Abdominal Aortic Aneurysm Expansion Using Longitudinal Data[J/OL]. Frontiers in Physics, 202 0, 7: 235. DOI:10.3389/fphy.2019.00235.

[14] Cyron C J, Aydin R C, Humphrey J D. A homogenized constrained mixture (and m echanical analog) model for growth and remodeling of soft tissue[J/OL]. Biomechanic s and Modeling in Mechanobiology, 2016, 15(6): 1389-1403. DOI:10.1007/s10237-016 -0770-9.

[15] Braeu F A, Seitz A, Aydin R C, et al. Homogenized constrained mixture models for anisotropic volumetric growth and remodeling[J/OL]. Biomechanics and Modeling in Mechanobiology, 2017, 16(3): 889-906. DOI:10.1007/s10237-016-0859-1.

[16] Jamaleddin Mousavi S, Jayendiran R, Farzaneh S, et al. Coupling hemodynamics wit h mechanobiology in patient-specific computational models of ascending thoracic aorti

c aneurysms[J/OL]. Computer Methods and Programs in Biomedicine, 2021, 205: 106107. DOI:10.1016/j.cmpb.2021.106107.
[17] Jiang Z, Choi J, Baek S. Machine learning approaches to surrogate multifidelity Growth and Remodeling models for efficient abdominal aortic aneurysmal applications[J/OL]. Computers in Biology and Medicine, 2021, 133: 104394. DOI:10.1016/j.compbiomed.2021.104394.
[18] Peng C, He W, Huang X, et al. The study on the impact of AAA wall motion on the hemodynamics based on 4D CT image data[J/OL]. Frontiers in Bioengineering and Biotechnology, 2023, 11[2023-08-26]. https://www.frontiersin.org/articles/10.3389/fbioe.2023.1103905. DOI:10.3389/fbioe.2023.1103905.
[19] Gharahi H, Zambrano B A, Lim C, et al. On growth measurements of abdominal aortic aneurysms using maximally inscribed spheres[J/OL]. Medical Engineering & Physics, 2015, 37(7): 683-691. DOI:10.1016/j.medengphy.2015.04.011.
[20] Gasser T C, Ogden R W, Holzapfel G A. Hyperelastic modelling of arterial layers with distributed collagen fibre orientations[J/OL]. Journal of The Royal Society Interface, 2006, 3(6): 15-35. DOI:10.1098/rsif.2005.0073.
[21] Ghavamian A, Mousavi S J, Avril S. Computational Study of Growth and Remodeling in Ascending Thoracic Aortic Aneurysms Considering Variations of Smooth Muscle Cell Basal Tone[J/OL]. Frontiers in Bioengineering and Biotechnology, 2020, 8: 587376. DOI:10.3389/fbioe.2020.587376.
[22] Mousavi S J, Farzaneh S, Avril S. Patient-specific predictions of aneurysm growth and remodeling in the ascending thoracic aorta using the homogenized constrained mixture model[J/OL]. Biomechanics and Modeling in Mechanobiology, 2019, 18(6): 1895-1913. DOI:10.1007/s10237-019-01184-8.
[23] Laubrie J D, Mousavi S J, Avril S. About prestretch in homogenized constrained mixture models simulating growth and remodeling in patient-specific aortic geometries[J/OL]. Biomechanics and Modeling in Mechanobiology, 2022, 21(2): 455-469. DOI:10.1007/s10237-021-01544-3.
[24] van Disseldorp E M J, Petterson N J, van de Vosse F N, et al. Quantification of aortic stiffness and wall stress in healthy volunteers and abdominal aortic aneurysm patients using time-resolved 3D ultrasound: a comparison study[J/OL]. European Heart Journal - Cardiovascular Imaging, 2019, 20(2): 185-191. DOI:10.1093/ehjci/jey051.
[25] Peng C, Zou L, Hou K, et al. Material parameter identification of the proximal and distal segments of the porcine thoracic aorta based on ECG-gated CT angiography[J/OL]. Journal of Biomechanics, 2022, 138: 111106. DOI:10.1016/j.jbiomech.2022.111106.
[26] Polzer S, Gasser T C, Vlachovský R, et al. Biomechanical indices are more sensitive than diameter in predicting rupture of asymptomatic abdominal aortic aneurysms[J/OL]. Journal of Vascular Surgery, 2020, 71(2): 617-626.e6. DOI:10.1016/j.jvs.2019.03.051.
[27] Olson S L, Wijesinha M A, Panthofer A M, et al. Evaluating Growth Patterns of Abdominal Aortic Aneurysm Diameter With Serial Computed Tomography Surveillance[J/OL]. JAMA Surgery, 2021, 156(4): 363-370. DOI:10.1001/jamasurg.2020.7190.
[28] Metaxa E, Tzirakis K, Kontopodis N, et al. Correlation of Intraluminal Thrombus De

position, Biomechanics, and Hemodynamics with Surface Growth and Rupture in Abdominal Aortic Aneurysm—Application in a Clinical Paradigm[J/OL]. Annals of Vascular Surgery, 2018, 46: 357-366. DOI:10.1016/j.avsg.2017.08.007.

[29] Bluestein D, Dumont K, De Beule M, et al. Intraluminal thrombus and risk of rupture in patient specific abdominal aortic aneurysm – FSI modelling[J/OL]. Computer Methods in Biomechanics and Biomedical Engineering, 2009, 12(1): 73-81. DOI:10.1080/10255840802176396.

[30] Baek S, Arzani A. Current state-of-the-art and utilities of machine learning for detection, monitoring, growth prediction, rupture risk assessment, and post-surgical management of abdominal aortic aneurysms[J/OL]. Applications in Engineering Science, 2022, 10: 100097. DOI:10.1016/j.apples.2022.100097.

[31] Zhang L, Jiang Z, Choi J, et al. Patient-Specific Prediction of Abdominal Aortic Aneurysm Expansion Using Bayesian Calibration[J/OL]. IEEE Journal of Biomedical and Health Informatics, 2019, 23(6): 2537-2550. DOI:10.1109/JBHI.2019.2896034.

[32] Xu J, Shi G P. Vascular wall extracellular matrix proteins and vascular diseases[J/OL]. Biochimica et Biophysica Acta (BBA) - Molecular Basis of Disease, 2014, 1842(11): 2106-2119. DOI:10.1016/j.bbadis.2014.07.008.

[33] Weiss D, Rego B V, Cavinato C, et al. Effects of Age, Sex, and Extracellular Matrix Integrity on Aortic Dilatation and Rupture in a Mouse Model of Marfan Syndrome [J/OL]. Arteriosclerosis, Thrombosis, and Vascular Biology, 2023: ATVBAHA.123.319122. DOI:10.1161/ATVBAHA.123.319122.

[34] Doyle B J, Callanan A, Burke P E, et al. Vessel asymmetry as an additional diagnostic tool in the assessment of abdominal aortic aneurysms[J/OL]. Journal of Vascular Surgery, 2009, 49(2): 443-454. DOI:10.1016/j.jvs.2008.08.064.

[35] Vorp D A, Raghavan M L, Webster M W. Mechanical wall stress in abdominal aortic aneurysm: Influence of diameter and asymmetry[J/OL]. Journal of Vascular Surgery, 1998, 27(4): 632-639. DOI:10.1016/S0741-5214(98)70227-7.

[36] Zeinali-Davarani S, Raguin L G, Vorp D A, et al. Identification of in vivo material and geometric parameters of a human aorta: toward patient-specific modeling of abdominal aortic aneurysm[J/OL]. Biomechanics and Modeling in Mechanobiology, 2011, 10(5): 689-699. DOI:10.1007/s10237-010-0266-y.

[37] Farsad M, Zeinali-Davarani S, Choi J, et al. Computational Growth and Remodeling of Abdominal Aortic Aneurysms Constrained by the Spine[J/OL]. Journal of Biomechanical Engineering, 2015, 137(091008)[2023-08-26]. https://doi.org/10.1115/1.4031019. DOI:10.1115/1.4031019.

[38] Horvat N, Virag L, Karšaj I. Mechanical role of intraluminal thrombus in aneurysm growth: A computational study[J/OL]. Biomechanics and Modeling in Mechanobiology, 2021, 20(5): 1819-1832. DOI:10.1007/s10237-021-01478-w.

[39] Virag L, Horvat N, Karšaj I. A computational study of bio-chemo-mechanics of thrombus-laden aneurysms[J/OL]. Journal of the Mechanics and Physics of Solids, 2023, 171: 105140. DOI:10.1016/j.jmps.2022.105140.

[40] Kessler V, Klopf J, Eilenberg W, et al. AAA Revisited: A Comprehensive Review of Risk Factors, Management, and Hallmarks of Pathogenesis[J/OL]. Biomedicines, 2022, 10(1): 94. DOI:10.3390/biomedicines10010094.

[41] Humphrey J D, Holzapfel G A. Mechanics, mechanobiology, and modeling of human abdominal aorta and aneurysms[J/OL]. Journal of Biomechanics, 2012, 45(5): 805-814. DOI:10.1016/j.jbiomech.2011.11.021.

Supplementary Files

This is a list of supplementary files associated with this preprint. Click to download.

- SupplementaryMaterial.docx